PERSPECTIVE • OPEN ACCESS

Synthetic criticality in cellular brains

To cite this article: Ricard Solé *et al* 2021 *J. Phys. Complex.* **2** 041001

View the article online for updates and enhancements.

Journal of Physics: Complexity

PERSPECTIVE

Synthetic criticality in cellular brains

Ricard Solé[1,2,3,*] , Nuria Conde-Pueyo[1,2], Antoni Guillamon[4,5,6], Victor Maull[1,2],
Jordi Pla[1,2] , Josep Sardanyés[5] and Blai Vidiella[1,2]

1. ICREA-Complex Systems Lab, Universitat Pompeu Fabra, 08003 Barcelona, Spain
2. Institut de Biologia Evolutiva (CSIC-UPF), 08003 Barcelona, Spain
3. Santa Fe Institute, 1399 Hyde Park Road, Santa Fe, NM 87501, United States of America
4. Departament de Matemàtiques, EPSEB, Universitat Politècnica de Catalunya, 08028 Barcelona, Spain
5. Centre de Recerca Matemàtica. Edifici C, Campus de Bellaterra, 08193 Cerdanyola del Vallès, Barcelona, Spain
6. Institut de Matemàtiques de la UPC-BarcelonaTech (IMTech), Universitat Politècnica de Catalunya, 08028 Barcelona, Spain
* Author to whom any correspondence should be addressed.
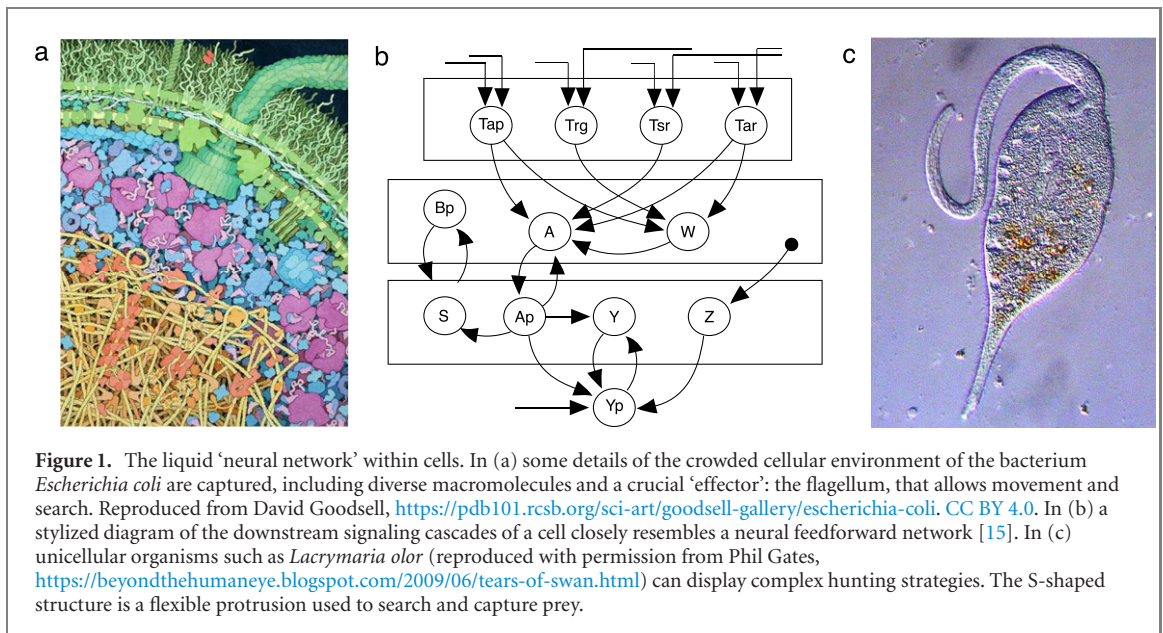
E-mail: ricard.sole@upf.edu

Abstract

Cognitive networks have evolved to cope with uncertain environments in order to make reliable decisions. Such decision making circuits need to respond to the external world in efficient and flexible ways, and one potentially general mechanism of achieving this is grounded in critical states. Mounting evidence has shown that brains operate close to such critical boundaries consistent with self-organized criticality (SOC). Is this also taking place in small-scale living systems, such as cells? Here, we explore a recent model of engineered gene networks that have been shown to exploit the feedback between order and control parameters (as defined by expression levels of two coupled genes) to achieve an SOC state. We suggest that such SOC motif could be exploited to generate adaptive behavioral patterns and might help design fast responses in synthetic cellular and multicellular organisms.

1. Introduction

The relevance of criticality in complex systems is well exemplified by the dynamics exhibited by brains and brain cell cultures that is consistent with the presence of a self-organized critical state [1–4]. In this context, it was early conjectured that systems performing computations could highly benefit from operating close to phase transition points [5]. On the other hand, a dynamical view of such an advantage emerges from considering the need for fast responses to changing conditions in a fluctuating environment [6]. Flocks of birds and fish schools, for example, would also be organized as a class of active matter where local interactions operate in such a way that cohesive group order coexists with rapid collective responses stemming from external inputs such as the presence of predators [7–9]. Finally, criticality might also be a useful dynamical state to perform efficient collective tasks in ant and termite colonies to execute colony-level computations [10, 11].

While brain criticality is tied to the dynamics of large, interconnected networks of neurons, cognition itself is not limited to standard neural masses. At the other extreme of the complexity spectrum, the so called *aneural* (no neurons) systems, including in particular single-cell organisms, share a number of commonalities with complex neural agents. As it has been pointed out by several authors they can exhibit complex behavior thanks to arrays of receptors that gather information from the outside world and a no less complex network of downstream molecular cascades that provide the processing requirements to make decisions. By contrast with 'solid' brains [12, 13] where the basic units (neurons) are located in given spatial locations and connected by a web of synaptic contacts, the inside of a cell (figure 1(a)) is a fluid, noisy and heterogeneous environment. Despite this apparent disorder, cells act as well-organized agents capable of properly and accurately respond to environmental uncertainty. This occurs thanks to the presence of information processing networks (figure 1(b)) that are, in many ways, not much different to well-known neural network models [14–16].

To some extent, we can talk about a 'liquid' cellular brain where the process of information takes place in a spatially distributed manner under molecular interactions involving, as with neural networks, threshold-like

Figure 1. The liquid 'neural network' within cells. In (a) some details of the crowded cellular environment of the bacterium *Escherichia coli* are captured, including diverse macromolecules and a crucial 'effector': the flagellum, that allows movement and search. Reproduced from David Goodsell, https://pdb101.rcsb.org/sci-art/goodsell-gallery/escherichia-coli. CC BY 4.0. In (b) a stylized diagram of the downstream signaling cascades of a cell closely resembles a neural feedforward network [15]. In (c) unicellular organisms such as *Lacrymaria olor* (reproduced with permission from Phil Gates, https://beyondthehumaneye.blogspot.com/2009/06/tears-of-swan.html) can display complex hunting strategies. The S-shaped structure is a flexible protrusion used to search and capture prey.
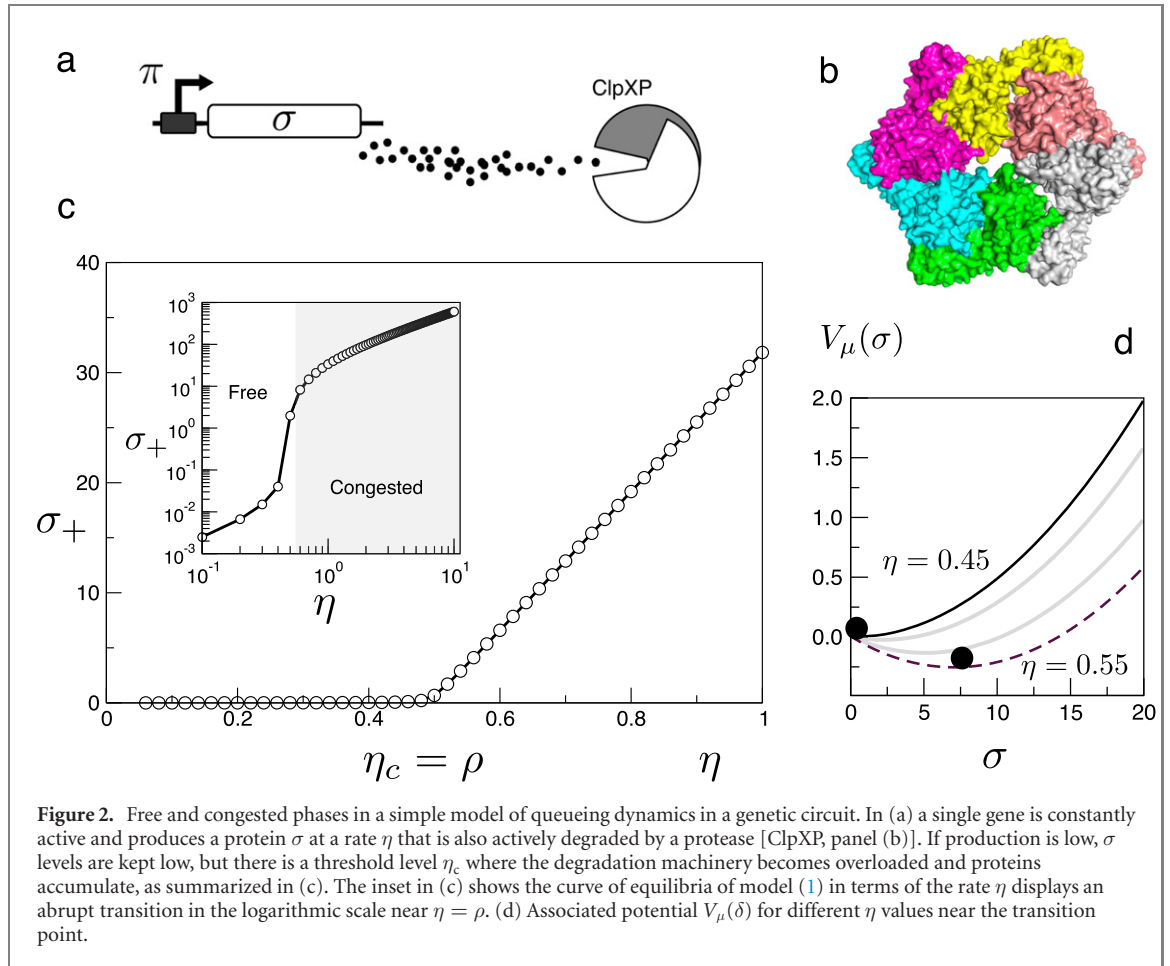
functions. Early work based on microscopic observations of single cell organisms by Binet [17] and Jennings [18] supported the concept that some kind of cellular intelligence could be defined, particularly obvious in those tasks involving movement towards food or away from harmful toxins. Such behavioral patterns necessarily involve internal states, error perception (and correction) or learning. Beyond the metaphor, the neural network analogy has been explicitly suggested within the context of microbial behavior [19]. The differences between unicellular and multicellular organisms are considerable, starting from the fact that the former necessarily communicate by means of diffusion processes, whereas diffusion cannot be used as a reliable way of coordination in the later. The invention of neurons has much to do with the need for efficiently and directionally send messages across a cohesive, physically connected cell assembly. And yet, unicellular agents can also rapidly respond to external signals.

Since critical states seem to be present in cortical systems and play a functional role, it is worth considering the possibility that self-organized criticality (SOC) might also be present in these fluid, cellular brains. In this paper we further explore this possibility, that has been recently raised in a study showing that SOC genetic circuits can be designed and implemented in living cells [20]. The origins of this SOC state are here analyzed under a deterministic framework, showing that the model genetic circuit contains the right ingredients for a self-organized state, namely a feedback between order and control parameters, responsible for the generation of fat-tailed distributions of gene expression under stochasticity. Potential applications of this SOC circuit are suggested within the context of behavioral patterns and the evolutionary and computational implications are outlined.

2. Cell congestion: free and jammed phases

Our starting point makes a connection with one of the classic topics of SOC within statistical physics of complexity: traffic congestion. One of the classic examples of critical phenomena in complex systems is the Nagel–Schreckenberger model of freeway traffic [21–23]. This model revealed the presence of a phase transition between laminar flow and start-stop-waves separated by point of maximum flow separating the two phases. The model, despite its simplicity, was also shown to match real traffic behavior. At criticality, wide fluctuations emerged. As discussed in this section, a similar scenario can be found (or engineered) within living cells.

How can bursting, self-organized critical states be generated inside single cells? The key requirement is to have a dynamical mechanism that exploits the tendency of a given genetic circuit to slowly increase gene expression levels (as grains of sand are added to a sandpile) until some negative feedback resets the state of the system. In order to create such a circuit, we start from a simpler model based on standard queueing transitions. In a previous study [24] it was shown how such a system can be defined, with the basic architecture as displayed in figure 2(a). It involves the constitutive (i.e. constant, non-regulated) expression of a gene coding for a protein, labeled σ. The degradation of σ takes place both spontaneously and as a result of the cellular proteolytic machinery [25], driven by means of the so called ClpXP protease (figure 2(b)). A simple model describing the

Figure 2. Free and congested phases in a simple model of queueing dynamics in a genetic circuit. In (a) a single gene is constantly active and produces a protein σ at a rate η that is also actively degraded by a protease [ClpXP, panel (b)]. If production is low, σ levels are kept low, but there is a threshold level η_c where the degradation machinery becomes overloaded and proteins accumulate, as summarized in (c). The inset in (c) shows the curve of equilibria of model (1) in terms of the rate η displays an abrupt transition in the logarithmic scale near $\eta = \rho$. (d) Associated potential $V_\mu(\delta)$ for different η values near the transition point.

dynamics of protein σ follows a deterministic (mean-field) system, given by the differential equation:

$$\frac{d\sigma}{dt} = \eta - \delta\sigma - \frac{\rho\sigma}{K + \sigma} =: f_\mu(\sigma), \tag{1}$$

where μ indicates the set of parameters (η, δ, ρ, K). These parameters indicate: the efficiency η of the (constitutive) expression of σ, its spontaneous decay rate δ, the active degradation rate ρ associated to the proteolytic machinery, and the Michaelis–Menten constant K. This model has a single attractor, namely

$$\sigma_+ = \frac{1}{2\delta}\left(\eta - \rho - K\delta + \sqrt{(\eta - \rho)^2 + K\delta(2\eta + 2\rho + K\delta)}\right), \tag{2}$$

which will always be stable since the sign of

$$\lambda(\sigma_+) = \frac{d}{d\sigma}f_\mu(\sigma_+) = -\delta - \frac{\rho K}{(K + \sigma_+)^2} \tag{3}$$

is always negative.

As we can see, this is not a standard phase transition (bifurcation) involving two fixed points whose stability is exchanged at criticality. Specifically, there is no phase involving an absorbing state, as it occurs with simple models of excitable dynamics [4]. This is summarized in figure 2(c), where we plot σ_+ against η. In the linear scale plot the system apparently displays a continuous phase transition (a transcritical bifurcation) but it obviously does not (given the presence of a single fixed point) and this is displayed in the inset with the log–log plot. The reason for this is that the constant inflow of particles does not allow trivial (zero activity) states to occur.

These two regimes can be qualitatively inferred. For $K \to 0$ (a scenario relevant to the synthetic implementations) we have

$$\left(\frac{d\sigma}{dt}\right)_{K\to 0} \approx \eta - \delta\sigma - \rho \tag{4}$$

with a fixed point

$$\sigma_+ = \frac{\eta - \rho}{\delta} \tag{5}$$

indicating that σ_+ will be zero for $\eta < \rho$, and grow linearly as $\sigma_+ \sim \eta/\delta$ with η. The non-critical character of the system is highlighted by looking at the associated potential $V_\mu(\sigma)$, defined from the condition $d\sigma/dt = -dV_\mu(\sigma)/d\sigma$ i.e. from

$$V_\mu(\sigma) = -\int f_\mu(\sigma)d\sigma = (\rho - \eta)\sigma + \frac{\delta}{2}\sigma^2 - \rho K \ln(K + \sigma) \tag{6}$$

and displayed in figure 2(d) for different values of η close to the threshold value $\eta_c = \rho = 0.5$. The shape of the potential does not allow to create the flattened valley close to η_c and no fat-tailed distributions will be observed in the stochastic counterpart. In this context, although some other traits, such as latency times, do display scaling laws close to the η_c boundary, no bursting avalanche dynamics will be observed. Can the presence of two distinct regimes be exploited to create a self-organized critical state? Work on statistical physics of self-organized critical traffic [26, 27] suggests a positive answer.

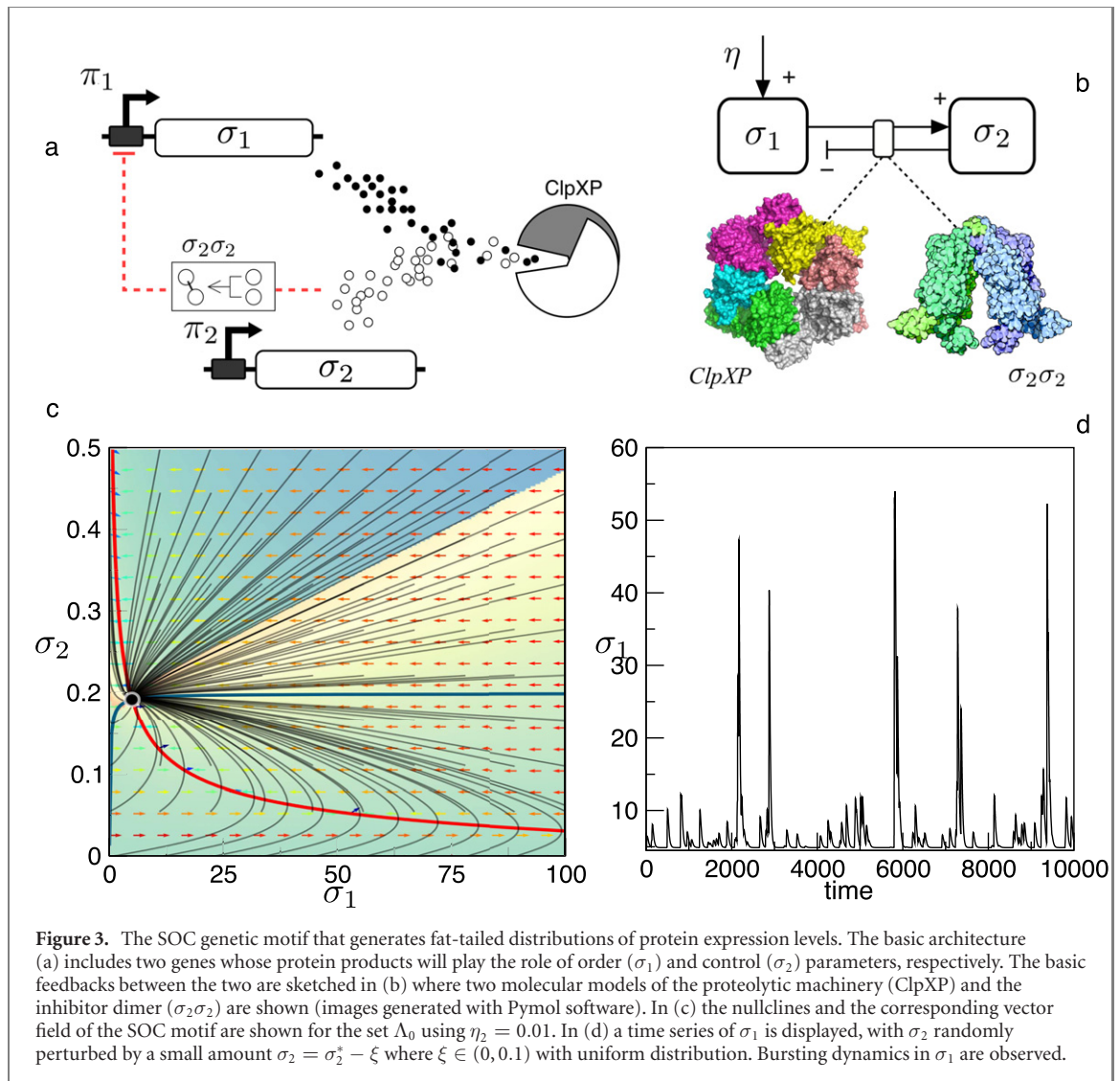## 3. Self-organized critical gene networks

The standard picture of SOC incorporates the concept of a feedback loop between order and control parameters in such a way that a complex system can evolve towards a second-order phase transition [28–30]. In this self-organized regime, the propagation of interactions among system components can lead to power law distributions of events. Most of the time, the system operates under a low-activity basis but very large events can be triggered due to the intrinsic excitability that is characteristic of criticality. As a result, SOC states would pervade a number of adaptive properties, including fast responses and maximal information processing. Here a critical point is an 'attractor', meaning that the system poises itself close to the transition boundary. In the canonical picture (such as the rice pile) as the system enters into the dynamical regime where avalanches are generated, the order parameter will exhibit critical fluctuations [31, 32]. In this case, it would be the angle of repose θ_c (as discussed in reference [20]). Each time an avalanche occurs, the slope θ can decrease below the critical θ_c control parameter, which will then start to grow back towards θ_c as new sand grains are slowly added to the pile.

Are there genetic circuits within cells operating in a SOC state? Could such dynamical states have played a key role in evolving cell-level cognitive complexity? Transcriptional bursting has been shown to play a relevant role in eukaryotic systems across multiple scales [34]. Here bursting allows information transmission in a digital fashion, while regulatory strength is encoded in the frequency of the fluctuations, although not necessarily connected to criticality. Some indirect observations suggest that SOC dynamics might occur in enzymatic networks [33]. An alternative path to explore these questions is to engineer SOC circuits using synthetic biology, as the one explored here [20] that allows to obtain SOC from the previous single-gene congestion model.

3.1. SOC network motif: deterministic properties

The basic architecture of the SOC motif is displayed in figure 3(a). The first gene expressing σ_1 is now degraded in competition with another protein σ_2 coded by another gene. Both genes are constitutively expressed: they are constantly expressing their respective proteins at rates that are defined by the binding properties of their promoters (π_1 and π_2). The efficiency of protein production can be properly tuned to guarantee that concentrations of both gene products are enough for the motif to be functional. Additionally, when the concentration is high enough, the protein monomers σ_2 form dimers, indicated as $\sigma_2\sigma_2$. Under this form, the protein complex represses the expression of σ_1. This implies a threshold condition: while concentrations are low, no dimers will be formed, but once congestion starts to emerge, σ_2 acts as a proper controller, reducing the expression of σ_1 to low levels. In this way we introduce the required negative loop from control to order parameter [35]. This is summarized in figure 3(b) where the qualitative nature of the interactions is indicated. Here, the constitutive production of σ_1 (the order parameter gene) acts as the driving constant that pushes up the expression level of this protein. Its increase causes congestion and raises the levels of σ_2 (since it cannot be properly degraded). As a consequence, dimers get formed and the negative feedback emerges.

This theoretical design was experimentally implemented using *E. coli* strains and fluorescent proteins (green and red fluorescent proteins, GFP and RFP, respectively) were used as reporters to track the expression levels of both σ_1 and σ_2. It was shown that, under a broad range of conditions, the feedback described here was able to generate a population-level pattern consistent with a SOC state. Using standard genetic engineering tools, the engineered parts were introduced into a single plasmid and the expression levels for each cell monitored by means of flow cytometry [20]. From these data sets, the levels of GFP displayed by a population of bacterial cells at a given time were shown to be power-law distributed. The design principle adopted in this motif is captured by a two-dimensional system of nonlinear ordinary differential equations describing the coupling

Figure 3. The SOC genetic motif that generates fat-tailed distributions of protein expression levels. The basic architecture (a) includes two genes whose protein products will play the role of order (σ_1) and control (σ_2) parameters, respectively. The basic feedbacks between the two are sketched in (b) where two molecular models of the proteolytic machinery (ClpXP) and the inhibitor dimer ($\sigma_2\sigma_2$) are shown (images generated with Pymol software). In (c) the nullclines and the corresponding vector field of the SOC motif are shown for the set Λ_0 using $\eta_2 = 0.01$. In (d) a time series of σ_1 is displayed, with σ_2 randomly perturbed by a small amount $\sigma_2 = \sigma_2^* - \xi$ where $\xi \in (0, 0.1)$ with uniform distribution. Bursting dynamics in σ_1 are observed.

between the order (σ_1) and the control (σ_2) parameters required to obtain criticality:

$$\frac{d\sigma_1}{dt} = f(\sigma_2) - \delta_1\sigma_1 - \sigma_1\Gamma(\sigma_1, \sigma_2), \tag{7}$$

$$\frac{d\sigma_2}{dt} = \eta_2 - \delta_2\sigma_2 - \sigma_2\Gamma(\sigma_1, \sigma_2), \tag{8}$$

where the following Hill function [35] is used:

$$f(\sigma_2) = \frac{\eta_1}{\theta + \sigma_2^2}, \tag{9}$$

for the repression mediated by $\sigma_2\sigma_2$ dimers. When σ_2 is small (the ClpXP system is working far from congestion) we have a production rate $f(\sigma_2 \to 0) \approx \eta_1/\theta$. The inhibition function has a threshold value θ representing the concentration σ_2^* at which the rate drops to half its maximum value i.e. $f(\sigma_2^*) = \eta_1/(2\theta)$. For larger values, it rapidly decays to zero. The saturation function, namely:

$$\Gamma(\sigma_1, \sigma_2) = \frac{\delta_c C}{K + \sigma_1 + \sigma_2}, \tag{10}$$

introduces the competition of both proteins for the proteolytic machinery. When no congestion occurs (due to low concentrations of both σ_1 and σ_2) we obtain a constant removal rate proportional to the concentration of ClpXP units, i.e. $\Gamma(0, 0) = \delta_c C/K$.

The SOC motif model displays (as desired) a single attractor within the meaningful domain defined by the non-negative concentration space, namely

$$\Omega_1 = \{(\sigma_1, \sigma_2) : \sigma_1 \geqslant 0, \sigma_2 \geqslant 0\}.$$

Intuitively, we can see that the saturation term forbids the possibility that the system grows in unbounded ways, whereas the input terms do not allow 'exclusion states' (with one of the species vanishing). The single fixed point (σ_1^*, σ_2^*) is obtained from the intersection of the nullclines obtained from $d\sigma_1/dt = d\sigma_2/dt = 0$ (see figure 3(c)). Although we have several parameters, as defined by the parameter set

$$\mathbf{\Lambda} := (\eta_1, \eta_2, \theta, \delta_1, \delta_2, \delta_c, C, K, \mu).$$

In our previous work [20], we fixed most of the parameters accordingly to well established estimates. Here we use the same data set with the specific values: $\mathbf{\Lambda}_0 = (10^{-2}, \eta_2, 10^{-3}, 5 \times 10^{-2}, 5 \times 10^{-2}, 10^{-1}, 10^{-1}, 10^{-3}, 1)$. The behavior was shown to be rather robust, with parameter η_2 requiring a minimal level in order to guarantee that the inhibitory regulation works. This can be analyzed by computing the eigenvalues of the Jacobian $J(\sigma^*)$ of our SOC motif system, given by

$$J(\sigma^*) = \left(\frac{\partial \dot{\sigma}_i}{\partial \sigma_j}\right)_{\sigma^*} = \begin{pmatrix} -\delta_1 - \Gamma + \sigma_1 \Gamma & \dfrac{-2\,\eta_1\,\sigma_2}{(\theta + \sigma_2^2)^2} + \sigma_1 \Gamma \\[12pt] \sigma_2\,\Gamma & -\delta_2 - \Gamma + \sigma_2 \Gamma \end{pmatrix}_{\sigma^*}, \tag{11}$$

with $\Gamma = \Gamma(\sigma_1, \sigma_2)$. These eigenvalues have always a negative real part, and they also display interesting properties as η_2 is increased [20]. In particular, it was shown that some statistical properties displayed by the stochastic counterpart (see below) were captured by the deterministic description. An example is the presence of a maximal variance in the distribution that occurs at a given η_2^c rate and that is connected with the transition between a stable node and a stable focus.

The shape of the nullclines and the underlying vector field allow to predict that variations in the control parameter σ_2 can cause wide changes in the order parameter σ_1, as desired. Starting from the fixed point σ^*, perturbations in σ_1 push the system within a domain of the phase portrait where a rapid growth in σ_1 occurs before it returns back to equilibrium. An example of this is shown in figure 3(d), where random, finite shifts in σ_2 are introduced at random times using the parameters from the set $\mathbf{\Lambda}_0$ and $\eta_2 = 0.01$. Fast, broad fluctuations are clearly appreciated. What is the statistical pattern displayed by these fluctuations?

3.2. Gene expression avalanches: stochastic dynamics

The experimental implementation of the previous motif (with some specific additions required to properly test the model and its parameter dependencies) revealed that power laws in the expression pattern of $\sigma_1 = [GFP]$ are indeed observable. Here the state of each cell is gathered from a cell population sample (after a transient time) and the cells flow (one cell at a time) through a laser beam. Thanks to the specific fluorescent label (green and red, in our case) light is absorbed and then emitted in a band of wavelengths and the intensity of each selected wavelength measured for each cell.

Cumulative plots were used: if $P(\sigma_1)$ indicates the probability distribution, the cumulative distribution is defined as $P_>(\sigma_1) = \int_0^{\sigma_1} P(\sigma) dP(\sigma)$. For our system, we obtained $P_>(\sigma_1) \sim \sigma_1^{-2}$. Since the time scale for cell division is short (comparable with the bursting dynamics scale) no time series were available, and thus we implicitly assume ergodicity: the time snapshot provided by the flow cytometry data should match the time evolution of the system. An example of these distributions is shown in figure 4(a).

The experimental results matched the predicted statistics obtained from the stochastic version of the SOC motif, as displayed in figure 4(a). The model described above can be stochastically implemented using a Gillespie algorithm [36]. The result reveals that, once the concentration required for σ_2 (the feedback loop from the control parameter) reaches a sufficiently high threshold, gene expression avalanches occur resulting in a power law [20], as the one shown in figure 4(b) that gives the same distribution. These fat-tailed distributions actually become dominant in a very large domain of the parameter space.
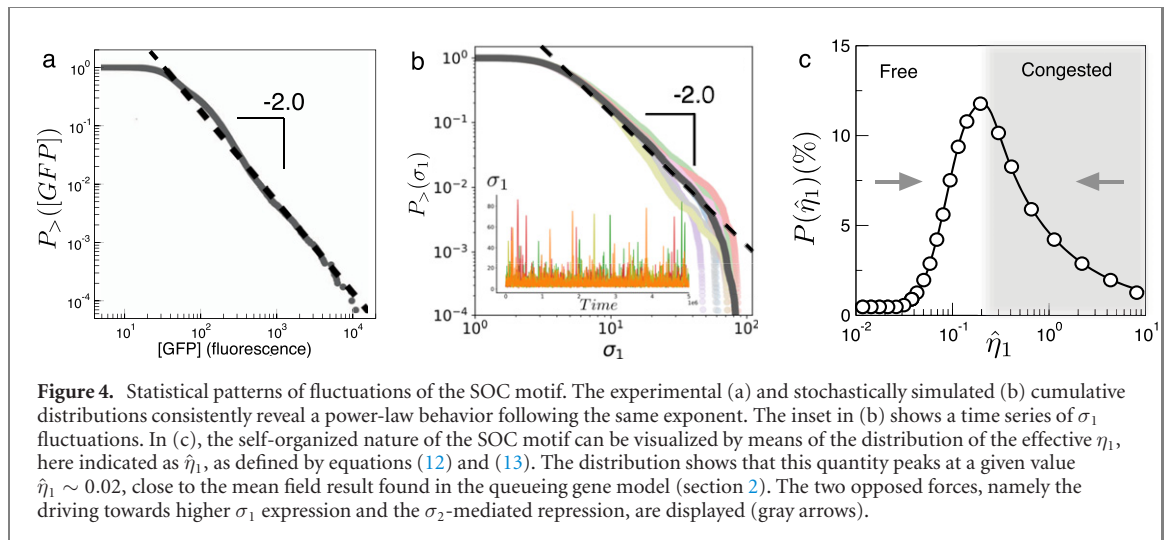
The spontaneous tendency toward criticality can be illustrated by considering a further simplification of the dynamical model. Consider the approximation $d\sigma_2/dt \approx 0$, i.e. that its dynamics if much faster than the one associated with the order parameter. In this case, we can re-write the SOC motif dynamics as follows:

$$\frac{d\sigma_1}{dt} = \hat{\eta}_1 - \delta_1 \sigma_1 - \sigma_1 \frac{\delta C}{K + \sigma_1 + \sigma_2}, \tag{12}$$

where we introduce a time-dependent function:

$$\hat{\eta}_1 = f(\sigma_2) = \frac{\eta_1}{\theta + \sigma_2^2}. \tag{13}$$

This captures the changes in the fluctuations in the driving rate associated with the order parameter resulting from the functional form associated to the control parameter. As defined, we have in fact transformed the

Figure 4. Statistical patterns of fluctuations of the SOC motif. The experimental (a) and stochastically simulated (b) cumulative distributions consistently reveal a power-law behavior following the same exponent. The inset in (b) shows a time series of σ_1 fluctuations. In (c), the self-organized nature of the SOC motif can be visualized by means of the distribution of the effective η_1, here indicated as $\hat{\eta}_1$, as defined by equations (12) and (13). The distribution shows that this quantity peaks at a given value $\hat{\eta}_1 \sim 0.02$, close to the mean field result found in the queueing gene model (section 2). The two opposed forces, namely the driving towards higher σ_1 expression and the σ_2-mediated repression, are displayed (gray arrows).

original two-dimensional model into a self-organized congestion model (similar to the one discussed before) where η_1 is now a self-tuned parameter that keeps adjusting itself as σ_2 fluctuates. By following the values of $\hat{\eta}_1$ and computing their frequency, a new distribution is obtained, and shown in figure 4(c). As expected for a SOC system, it shows a peak close to the boundary found for the single-gene queueing model, separating the free from the congested behavior except that, in this case, not such boundary exists.
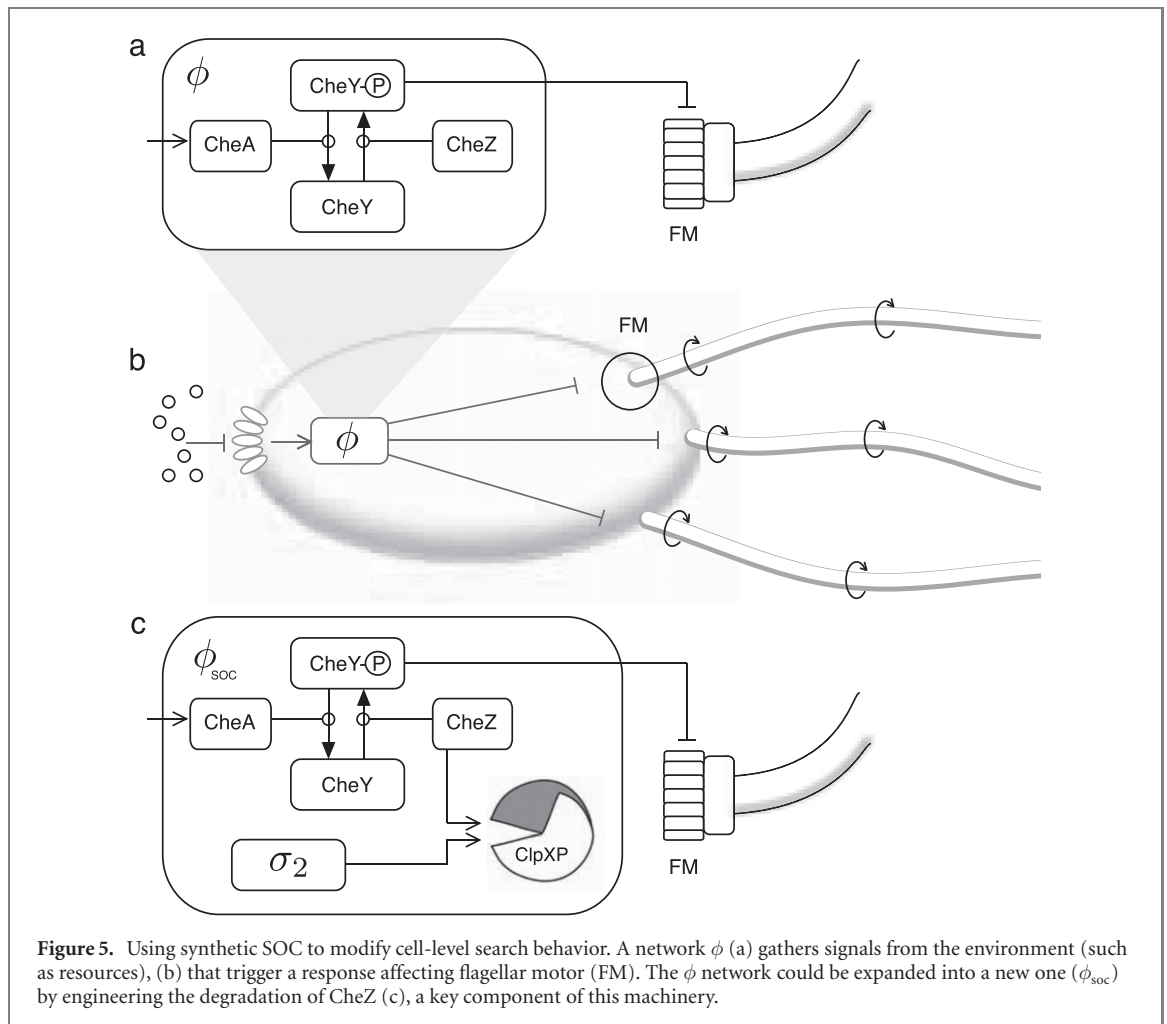
The engineering of SOC dynamics within living cells provides a proof of concept for the design of reliable gene circuits that can generate this fat-tailed class of noise. This is a first step that promises to expand our potential for designing nonlinear phenomena with features similar to those found in neural systems. How can this SOC motif principle be applied to tune cell behavior?

4. Using criticality to control cellular behavior

In order to adapt to environmental challenges, biological systems exhibit a diverse array of response mechanisms grounded in sensors and actuators as well as in information-processing units. Adaptive responses require dynamical features that combine low energetic costs along with fast changes to efficiently respond to environmental changes. Within cells, noise was early identified as playing multiple roles affecting cell fate, population heterogeneity, signal amplification or response to stress [37–39]. Noise is both an inevitable outcome of stochastic molecular interactions and an essential ingredient in decision making [40]. Several features of cell dynamics might result from criticality. One example is the complex dynamics of microtubules in eukaryotic cells [41–44]. In this case, the length and spatial distribution of these structures determine cell's shape and are crucial to cell motility, division, and intracellular transport. Both measured changes in microtubule length and their explanation in terms of statistical physics models support the concept that they operate in a dynamical instability state. In this, coevolution has acted as the mechanism that tuned the rates of molecular assembly and disassembly.

As pointed out at the beginning of this paper, single-celled organisms possess a broad repertoire of behavioral responses that allow them to navigate in changing environments. Bacteria such as *E. coli* detect and react to chemical gradients while paramecia or amoeba (eukaryotic organisms) are capable of rapidly reacting to currents and obstacles. Using criticality as a way of rapidly responding to stimuli could enhance the efficiency of such responses. In what ways our SOC motif could be used to *create* or modify cognitive tasks?

One possible way of using our SOC motif as a way to tune microbial behavior could involve a coupling between the two-gene network and the cellular machinery responsible for movement [45]. This machinery, as defined by a signaling network, is particularly well known in *E. coli*, where a group of signaling proteins are involved in the sensing of environmental cues, processing these as input signals and eventually acting on the flagella motor that is responsible for cell movement [46] (see figure 5). Specifically, the bacterium has a default direction of rotation, which is counterclockwise in *E. coli*. The flagellar motor always rotates counterclockwise unless the appropriate signal is sent. A group of signal transduction proteins {CheA, CheY, CheZ . . .} are involved. These proteins form a network motif ϕ (figures 5(a) and (b)) that includes the sensor, processing and effector steps required to connect environment and cell displacement. The concentrations of CheY and CheZ, in particular, are known to affect swimming behavior. High concentrations of an active form of ChezY (indicated as CheY-P in figure 5(a)) enhance tumbling whereas CheZ inhibits ChezY. As a consequence, we conjecture that using CheZ as our σ_1 component could allow to tune bacterial chemotaxis.

Figure 5. Using synthetic SOC to modify cell-level search behavior. A network ϕ (a) gathers signals from the environment (such as resources), (b) that trigger a response affecting flagellar motor (FM). The ϕ network could be expanded into a new one (ϕ_{soc}) by engineering the degradation of CheZ (c), a key component of this machinery.

The proposed extension of the SOC motif is summarized in figure 5(c): using CheZ as the order parameter and the SOC motif design for its control, the new circuit ϕ_{soc} would produce bursts in CheZ that should modify the pattern of flagella rotation. By tuning η_2, we would expect to see different movement patterns. This is an interesting scenario to test ideas concerning the search patterns of organisms that take advantage of given statistical regularities of fat-tailed distributions of jumps. If such tuning works, it would be possible to engineer different strains and perform competition experiments to test the hypothesis that critical dynamics can be an optimal solution to explore heterogeneous environments. This is a specially active area within the physics of complex systems known as active matter [47]. In general terms, this is a novel class of non-equilibrium materials made of a large number of energy-dependent units that display collective behavior. The study of the motion of living swarms in particular has been largely inspired by the study of the motion of ants, termites and microorganisms [48]. Swarms are known to display critical dynamics too, and our synthetic design could help explore the potential phases exhibited by possible (but not actual) classes of behavior. This will be particularly relevant if the SOC motif is extended towards cell–cell communication patterns.

Another application of the critical gene network concerns the engineering of bacteria used in some biomedical applications such as the detection and elimination of cancer cells [49, 50], a very active area within synthetic biology, which has taken advantage of nonlinear dynamical phenomena such as synchronization [51]. The key concept is that tumor-selective expression of a given gene can be placed under the control of some external signal that is associated to the presence of tumor populations. Examples of such signals characteristic of many tumors are the presence of hypoxia (i.e. reduced oxygen levels) or glucose gradients often found in solid tumors. Once the bacterium senses the right conditions (which could be threshold-level triggers) antitumour proteins can be expressed close to metabolically active regions of the tumor mass. Having a SOC motif coupled to such as sensor-actuator system would ensure a highly sensitive targeting of cancer cells. If such external drivers (perhaps affecting our candidate σ_1 factor) are absent, low levels of delivery of therapeutic payloads would be expected, thus limiting potential cytotoxic effects on normal tissue. As soon as the engineered cell gets closer to the target tumor, the high excitability of the SOC motif would lead to bursting episodes of release, which could drive to cell death. Under this scenario, as cells burst, they deliver the anticancer agents.

There is a potentially broad range of situations where our critical motif can play a useful role closer to the one found in neural networks. As we mentioned at the beginning, cellular circuits have been compared to neural networks, and the rich complexity of cellular webs should offer multiple possibilities to exploit our design principle.

5. Discussion

The idea that complex patterns of cellular behavior can be an emergent property of gene-gene interactions was early proposed by Stuart Kauffman, who used a Boolean approximation [52, 53]. This view was originated shortly after the classical work by Jacques Monod and François Jacob on the switching behavior of gene regulation [54]. It is interesting to notice that, since those early years, both neural and genetic networks have received increasing attention both at the level of the details of their interacting constituents as well as in terms of theoretical models. In both cases, response functions are typically stepwise. One particularly key result from the study of Boolean gene network dynamics was the presence of a critical transition associated to the attractor dynamics of differentiate states. It was found that a critical connectivity separating an ordered and a disordered phase allowed a limited set of robust cell states to exist [55–57]. As a consequence of this prediction, perturbations of genes should trigger cascades of changes affecting s genes following a critical branching process scaling $P(s) \sim s^{-3/2}$, as confirmed by knock-out data. Our SOC motif offers a new layer of complexity to this picture of cells as systems poised close to criticality.

Are SOC motifs likely to be present in cells? The basic components of the SOC design presented here are widespread in natural genetic regulatory networks. Many proteins are processed by the proteolytic machinery and most regulatory feedbacks involve dimerized complexes following the functional responses described above. The kind of critical circuit that we have discussed here should not only be possible: we conjecture that it might be present and future work should explore potential candidates and their potential relevance.

Our design principle could be translated into the multicellular domain. We have limited ourselves to single-cell dynamics, but engineering communication between cells is also easy to achieve and pervades the development of collective synthetic intelligence [58]. In this context, it has been shown that some simple (non-neural) organisms, such as Placozoans, exhibit criticality in their locomotion dynamics [59, 60]. Such kind of pattern could be also engineered in mammalian cells using our basic design principle. One candidate to this implementation are so called bio-robots [61, 62] which have been created by means of the assembly of different cell types from amphibians. Here one of the cell populations spontaneously exhibits excitable dynamics that allows the synthetic organisms to move in simple ways. Could a SOC motif including cell-cell communication allow them to display complex, adaptive search patterns closer to their natural counterparts? This possibility opens new avenues in the exploration of so called synthetic evolutionary transitions [63] and the understanding of the origins of early forms of cognition.

Data availability statement

No new data were created or analyzed in this study.

ORCID iDs

Ricard Solé https://orcid.org/0000-0001-6974-1008
Jordi Pla https://orcid.org/0000-0003-2388-9407
Josep Sardanyés https://orcid.org/0000-0001-7225-5158
Blai Vidiella https://orcid.org/0000-0002-4819-7047

References

[1] Chialvo D R 2004 Critical brain networks *Physica* A **340** 756–65
[2] Chialvo D R 2010 Emergent complex neural dynamics *Nat. Phys.* **6** 744–50
[3] Plenz D, Niebur E and Schuster H G 2014 *Criticality in Neural Systems* (New York: Wiley)
[4] Hesse J and Gross T 2014 Self-organized criticality as a fundamental property of neural systems *Front. Syst. Neurosci.* **8** 166
[5] Langton C G 1990 Computation at the edge of chaos: phase transitions and emergent computation *Physica* D **42** 12–37
[6] Mora T and Bialek W 2011 Are biological systems poised at criticality? *J. Stat. Phys.* **144** 268–302
[7] Bartumeus F 2007 Lévy processes in animal movement: an evolutionary hypothesis *Fractals* **15** 151–62
[8] Bialek W, Cavagna A, Giardina I, Mora T, Pohl O, Silvestri E, Viale M and Walczak A M 2014 Social interactions dominate speed control in poising natural flocks near criticality *Proc. Natl Acad. Sci.* **111** 7212–7
[9] Couzin I D 2018 Synchronization: the key to effective communication in animal collectives *Trends Cognit. Sci.* **22** 844–6
[10] Solé R V and Miramontes O 1995 Information at the edge of chaos in fluid neural networks *Physica* D **80** 171–80
[11] Miramontes O 1995 Order–disorder transitions in the behavior of ant societies *Complexity* **1** 56–60
[12] Solé R, Moses M and Forrest S 2019 Liquid brains, solid brains *Phil. Trans. R. Soc.* B **374** 20190040
[13] Piñero J and Solé R 2019 Statistical physics of liquid brains *Phil. Trans. R. Soc.* B **374** 20180376
[14] Bray D 1990 Intracellular signalling as a parallel distributed process *J. Theor. Biol.* **143** 215–31
[15] Bray D 1995 Protein molecules as computational elements in living cells *Nature* **376** 307–12
[16] Bray D 2009 *Wetware* (*A Computer in Every Living Cell*) (New Haven, CT: Yale University Press)
[17] Binet A 1888 *The Psychic Life of Micro-organisms* (Chicago: Open Court)
[18] Jennings H S 1905 *Behavior of the Lower Organisms* (Bloomington, IN: Indiana University Press)
[19] Armitage J P, Holland I B, Jenal U and Kenny B 2005 'Neural networks' in bacteria: making connections *J. Bacteriol.* **187** 26–36
[20] Vidiella B, Guillamon A, Sardanyés J, Maull V, Pla J, Conde N and Solé R 2021 Engineering self-organized criticality in living cells *Nat. Commun.* **12** 4415
[21] Nagel K and Schreckenberg M 1992 A cellular automaton model for freeway traffic *J. Phys.* I **2** 2221–9
[22] Nagel K and Rasmussen S 1994 Traffic at the edge of chaos *Artificial Life IV* ed R A Brooks and P Maes (Cambridge, MA: MIT Press) pp 222–35
[23] Helbing D 2001 Traffic and related self-driven many-particle systems *Rev. Mod. Phys.* **73** 1067
[24] Cookson N A, Mather W H, Danino T, Mondragón-Palomino O, Williams R J, Tsimring L S and Hasty J 2011 Queueing up for enzymatic processing: correlated signaling through coupled degradation *Mol. Syst. Biol.* **7** 561
[25] Gottesman S 2003 Proteolysis in bacterial regulatory circuits *Annu. Rev. Cell Dev. Biol.* **19** 565–87
[26] Solé R V and Valverde S 2001 Information transfer and phase transitions in a model of internet traffic *Physica* A **289** 595–605
[27] Guimerà R, Díaz-Guilera A, Vega-Redondo F, Cabrales A and Arenas A 2002 Optimal network topologies for local search with congestion *Phys. Rev. Lett.* **89** 248701
[28] Sornette D, Johansen A and Dornic I 1995 Mapping self-organized criticality onto criticality *J. Phys.* I **5** 325–35
[29] Jensen H J 1998 *Self-Organized Criticality* (*Emergent Complex Behaviour in Physical and Biological Systems*) (Cambridge: Cambridge University Press)
[30] Muñoz M A 2018 Colloquium: criticality and dynamical scaling in living systems *Rev. Mod. Phys.* **90** 031001
[31] Bak P, Tang C and Wiesenfeld K 1988 Self-organized criticality *Phys. Rev.* A **38** 364–74
[32] Christensen K and Moloney N 2005 *Complexity and Criticality* (London: Imperial College Press)
[33] Steiner P J, Williams R J, Hasty J and Tsimring L S 2016 Criticality and adaptivity in enzymatic networks *Biophys. J.* **111** 1078–87
[34] Wang Y, Ni T, Wang W and Liu F 2019 Gene transcription in bursting: a unified mode for realizing accuracy and stochasticity *Biol. Rev.* **94** 248–58
[35] Alon U 2019 *An Introduction to Systems Biology* (*Design Principles of Biological Circuits*) (Boca Raton, FL: CRC Press)
[36] Gillespie D T 1976 A general method for numerically simulating the stochastic time evolution of coupled chemical reactions *J. Comput. Phys.* **22** 403–34
[37] Rao C V, Wolf D M and Arkin A P 2002 Control, exploitation and tolerance of intracellular noise *Nature* **420** 231–7
[38] Raj A and van Oudenaarden A 2008 Nature, nurture, or chance: stochastic gene expression and its consequences *Cell* **135** 216–26
[39] Eldar A and Elowitz M B 2010 Functional roles for noise in genetic circuits *Nature* **467** 167–73
[40] Balázsi G, van Oudenaarden A and Collins J J 2011 Cellular decision making and biological noise: from microbes to mammals *Cell* **144** 910–25
[41] Howard J and Hyman A A 2003 Dynamics and mechanics of the microtubule plus end *Nature* **422** 753–8
[42] Antal T, Krapivsky P, Redner S, Mailman M and Chakraborty B 2007 Dynamics of an idealized model of microtubule growth and catastrophe *Phys. Rev.* E **76** 041907
[43] Antal T, Krapivsky P L and Redner S 2007 Dynamics of microtubule instabilities *J. Stat. Mech.* L05004
[44] Solé R 2011 *Phase Transitions* (Princeton, NJ: Princeton University Press)
[45] Adler J 1976 The sensing of chemicals by bacteria *Sci. Am.* **234** 40–7
[46] Eisenbach M 2011 Bacterial chemotaxis *Encyclopedia of Life Sciences* (Chichester: Wiley) https://doi.org/10.1002/9780470015902.a0001251.pub3
[47] Schweitzer F 2003 *Brownian Agents and Active Particles* (Berlin: Springer)
[48] Hu D L, Phonekeo S, Altshuler E and Brochard-Wyart F 2016 Entangled active matter: from cells to ants *Eur. Phys. J. Spec. Top.* **225** 629–49
[49] Chien T, Doshi A and Danino T 2017 Advances in bacterial cancer therapies using synthetic biology *Curr. Opin. Syst. Biol.* **5** 1–8
[50] Wu M R, Jusiak B and Lu T K 2019 Engineering advanced cancer therapies with synthetic biology *Nat. Rev. Cancer* **19** 187–95
[51] Din M O *et al* 2016 Synchronized cycles of bacterial lysis for *in vivo* delivery *Nature* **536** 81–5
[52] Kauffman S A 1969 Metabolic stability and epigenesis in randomly constructed genetic nets *J. Theor. Biol.* **22** 437–67
[53] Kauffman S A 1993 *Origins of Order* (New York: Oxford University Press)
[54] Jacob F and Monod J 1963 Genetic repression, allosteric inhibition, and cellular differentiation *Cytodifferentiation and Macromolecular Synthesis* vol 21 (New York: Academic) pp 30–64
[55] Serra R, Villani M, Graudenzi A and Kauffman S A 2007 Why a simple model of genetic regulatory networks describes the distribution of avalanches in gene expression data *J. Theor. Biol.* **246** 449
[56] Balleza E, Alvarez-Buylla E R, Chaos A, Kauffman S, Shmulevich I and Aldana M 2008 Critical dynamics in genetic regulatory networks: examples from four kingdoms *PLoS One* **3** e2456

[57] Daniels B C, Kim H, Moore D, Zhou S, Smith H B, Karas B, Kauffman S A and Walker S I 2018 Criticality distinguishes the ensemble of biological regulatory networks *Phys. Rev. Lett.* **121** 138102

[58] Solé R, Amor D R, Duran-Nebreda S, Conde-Pueyo N, Carbonell-Ballestero M and Montañez R 2016 Synthetic collective intelligence *Biosystems* **148** 47–61

[59] Davidescu M and Couzin I 2014 Transient leadership and collective cell movement in early diverged multicellular animals (arXiv:1407.0972)

[60] Smith C and Mayorova T 2019 Insights into the evolution of digestive systems from studies of Trichoplax adhaerens *Cell Tissue Res.* **377** 353–67

[61] Blackiston D, Lederer E, Kriegman S, Garnier S, Bongard J and Levin M 2021 A cellular platform for the development of synthetic living machines *Sci. Robot.* **6** eabf1571

[62] Ebrahimkhani Mo R and Levin M 2021 Synthetic living machines: a new window on life *Iscience* **24** 102505

[63] Solé R 2016 Synthetic transitions: towards a new synthesis *Phil. Trans. R. Soc.* B **371** 20150438